Meccanica (2006) 41:119–142
DOI 10.1007/s11012-005-0409-x

Frictional Oscillations Under the Action of Almost Periodic Excitation

K.V. AVRAMOV[1,*] and J. AWREJCEWICZ[2]
[1] *Department of Gas and Fluid Mechanics, National Technical University "Kharkov Polytechnic University", Frunze St.21, Kharkov 61002, Ukraine;* [2] *Department of Automatics and Biomechanics, Technical University of Lodz, 1/15 Stefanowskiego St., 90-924, Lodz, Poland, e-mail: awrejcew@p.lodz.pl*

(Received 30 April 2004; accepted in revised form: 13 May 2005)

Abstract. Frictional oscillations under the action of almost periodic force are studied. The modulation equations are derived by the multiple scales method to study bifurcations behavior. Heteroclinic Melnikov function is constructed to obtain the region of chaotic solutions of these equations. Bifurcations of almost periodic orbits are studied by Van der Pol transformation and averaging procedure.

Key words: Frictional oscillations, Heteroclinic orbits, Multiple scales method, Heteroclinic Melnikov function.

1. Introduction

The analysis of friction nonlinear oscillations has great importance in machine tools manufactures, polished plants, braking systems. Frictional auto-oscillations limit the operation of gyroscopic systems. Many efforts were made to study these problems. Den Hartog [1] considered string oscillations taking into account a bow moving on the string. Andronov *et al*. [2] considered oscillations with the decreasing part of the kinetic friction characteristic. Kauderer [3] noted that frictional auto-oscillations are the simplest model to explain acoustic phenomena. Frictional auto-oscillations of two moving body are considered by Kononenko [4]. He presented the experimental kinetic friction characteristics and the functions approximated these characteristics. The auto-oscillations excited by friction of moving belt and oscillating body are studied by Kononeko [5], Alifov and Frolov [6]. These authors consider the belt driving by the limited power supply. The autonomous stick-slip system is studied analytically by Popp and Stelter [7]. They considered chaotic oscillations of the periodically excited systems. The different forms of kinetic friction characteristics are suggested by Oestreich *et al*. [8] Feeny and Moon [9, 10] considered the dry friction oscillator with the normal force, which is proportional to the mass displacement. Wojewoda and Kapitaniak [11] Wojewoda *et al*. [12] obtained one-dimensional map to study a chaotic dynamics of the dry friction oscillator. Their numerical studies show, that

* Author for correspondence: e-mail: kvavr@kharkov.ua

the chaotic behavior arises as a result of the sequence of the period-doubling bifurcations. The system of two bodies coupled by dry friction under the action of the almost periodic force is studied experimentally in the papers [11, 12].

The stick-slip chaos has been discovered in one-degree-of-freedom system by Popp and Stelter [13]. It seems that the first report about the stick-slip chaotic behavior and a coexistence of various non-smooth regular and irregular attractors in the two degrees-of-freedom systems are reported by Awrejcewicz and Delfs [14, 15]. Since the mentioned papers are focused on a qualitative and quantitative analysis with a help of numerical approaches, an attempt to predict stick-slip chaos analytically is highly required. It is worth noticing that this problem is solved by Awrejcewicz and Holicke [16], where the Melnikov function for a stick-slip chaos exhibited in one degree-of-freedom non-autonomous system is constructed. The predicted analytically stick-slip chaos is verified through numerical computations showing a good coincidence. Awrejcewicz and Olejnik [17] studied recently a two degrees-of-freedom autonomous mechanical system consisted of two masses, where one of them lies on a moving belt with a constant velocity. Among classical approaches applied to analysis of the autonomous system (time histories, phase projections, Poincare maps, bifurcation diagrams, Lyapunov exponents, etc.), special attention is paid to application of both the modified Henon's numerical method (particularly suitable for a study of discontinuous systems) and of the Lagrange interpolation used to obtain the Lyapunov exponents in more efficient way than the standard approaches. In the paper [18], a special numerical algorithm is proposed to quantify regular and irregular dynamics directly without an application of the Lyapunov exponents concept. Its suitability to analyze stick-slip chaos is discussed and illustrated in the next works by Awrejcewicz and Dzyubak [19]. More complicated models of a real stick-slip behavior occurred in a frictional pairs accounting of thermal processes and wear are analyzed in the papers [20, 21]. Both theoretical background and numerous examples of regular and chaotic dynamics of discontinous mechanical systems including friction and impacts are reported in the book [22]. The results of the numerical simulations of the mass-spring system interacted with the moving belt are presented in the paper [23].

The mass oscillations in the clearance are studied by Balandin [24]. Frictional auto-oscillations of this system excited by the plate interacted with the mass. Marjuta [25] considered the nonlinear dynamic of the Froud pendulum. He showed that the experimental data disagree with the numerical simulations of the van der Pol equation. Therefore, Marjuta used another model of frictional interactions. The auto-oscillations of the Froud pendulum are considered in the book of Landa [26]. Pfeiffer [27] considers the dynamics of bodies with several frictional contacts with moving surfaces. This theory is used to analyze the drilling machine. Oscillations of the braking system, which is modeled by the self-excited nonlinear system, are studied by Sinou *et al*. [28, 29]. In this paper the center manifolds method is used to analyze the Hopf bifurcation. Many engineering applications of frictional auto-oscillations are presented in the book of Kragelskii [30]. The history of nonlinear systems with friction is reported by Feeny *et al*. [31].

Almost periodic forces are frequently encountered in engineering sciences. Nonlinear systems under the action of almost periodic forces are considered by Malkin [32]. Nayfeh and Mook [33] used the multiple scales method to analyze such systems. The quasilinear oscillator under the action of the almost periodic force is considered

by Vavriv *et al.* [34]. They derive the modulation equations of the main resonance, which contain the saddle point with two homoclinic orbits. The Duffing oscillator with two small parameters under the action of the almost periodic force is studied by Wiggins [35], Ide and Wiggins [36]. The unperturbed modulation equations of the Duffing oscillator contain the homoclinic orbits. Wiggins use the Melnikov method to analyze the homoclinic torus. Yagasaki [37] studies the Duffing oscillator under the action of the almost periodic excitation by the perturbation methods. He applies the Melnikov method to analyze the chaotic states of the modulation equations. The bifurcations of almost periodic motions are investigated by Yagasaki [38] too. The Duffing-van-der-Pol oscillator excited by the almost periodic force is considered by Yagasaki [39]. Nonlinear systems under the action of almost periodic forces are generalized by Wiggins [40].

The mass-spring nonlinear system interacting with a moving belt is considered in this paper. The oscillations excited by the almost periodic force are studied by the multiple scales method. The periodic motions and their bifurcations are investigated in the system of modulation equations. These equations are obtained by the multiple scales method. The heteroclinic Melnikov function is constructed to analyze the chaotic states of the modulation equations. The analytical results are compared with the data of the numerical simulations.

The novelty of the paper is application of the multiple scales method, Van-der-Pol transformation and Melnikov function to study the frictional oscillator under the action of the almost periodic force.

This paper is organized in the next form. The equations of mechanical system are presented in Section 2. The derivation of the modulation equations in the case of the resonance $\Omega_1 \approx 1$; $\Omega_2 \approx \Omega_1$ is reported in Section 3. The unperturbed system of the modulation equations ($\mu = 0$) is treated in Section 4. The Section 5 contains the analysis of almost periodic oscillations, which is reduced to the modulation equations. The analytical analysis of the heteroclinic Melnikov function of the modulation equations is presented in Section 6. Section 7 contains the results of the numerical simulations.

2. Equations of Motions

Figure 1 shows the considered system. The oscillations are described by the generalized coordinate x. The belt moving with constant velocity v_* interacts with the oscillator due to the friction force $f(v_R)$ (Figure 1b), where v_R is a relative velocity of the rubbing surfaces. The system excited by the almost periodic force $p(t) = \Gamma_1 \cos \omega_1 t + \Gamma_2 \cos \omega_2 t$. The spring is considered as nonlinear: $R = cx + c_3 x^3$. The differential equation of oscillations is the following:

$$\begin{aligned} &m\ddot{x} + cx + c_3 x^3 = \Gamma_1 \cos \omega_1 t + \Gamma_2 \cos \omega_2 t - f(\dot{x} - v_0), \\ &f(\dot{x} - v_0) = \theta_0 \ \mathrm{sign}(\dot{x} - v_0) - A(\dot{x} - v_0) + B(\dot{x} - v_0)^3. \end{aligned} \tag{1}$$

The following two small parameters are considered:

$$0 < \varepsilon \ll \mu \ll 1. \tag{2}$$

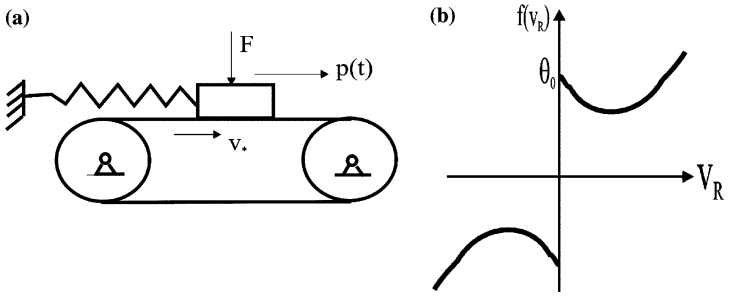

Figure 1. The mechanical system and a kinetic friction characteristics.

The dimensionless variables and parameters have the following form:

$$
\begin{aligned}
&x = x_0\xi(t), \quad \omega_0 = \sqrt{\frac{c}{m}}, \quad \tau = \omega_0 t, \quad \Omega_1 = \frac{\omega_1}{\omega_0}, \quad \Omega_2 = \frac{\omega_2}{\omega_0},\\
&\varepsilon\lambda = \frac{c_3 x_0^2}{c}, \quad \varepsilon\mu\tilde{\theta} = \frac{\theta_0}{cx_0}, \quad \varepsilon\gamma_1 = \frac{\Gamma_1}{cx_0},\\
&v_B = \frac{v_0}{x_0\omega_0}, \quad \varepsilon\mu\gamma_2 = \frac{\Gamma_2}{cx_0}, \quad \alpha = \frac{A\omega_0 x_0}{\theta_0}, \quad \beta = \frac{B\omega_0^3 x_0^3}{\theta_0}.
\end{aligned}
\tag{3}
$$

Equation (1) is written as

$$
\begin{aligned}
&\xi'' + \xi = \varepsilon\left\{-\lambda\xi^3 + \gamma_1\cos\Omega_1\tau + \mu\left[\gamma_2\cos\Omega_2\tau - \tilde{\theta}P(\xi' - v_B)\right]\right\},\\
&P(\xi' - v_B) = \ \mathrm{sign}(\xi' - v_B) - \alpha(\xi' - v_B) + \beta(\xi' - v_B)^3.
\end{aligned}
\tag{4}
$$

Note, that if the external excitation is absent in the system (4), the slipping mode predominates significantly over the sticking one and the motion is close to harmonic. It is well known that if the periodic force acts on the system (4), the rich bifurcations behavior takes place [8]. The analysis presented here is based on the assumption, that the friction force is small. Therefore, this force determines the modulations of oscillations and this force affects a little on the sine form of oscillations and the frequency.

3. Modulation Equations of Resonance $\Omega_1 \approx 1$, $\Omega_2 \approx \Omega_1$

The following resonance conditions are considered:

$$
\Omega_1 = 1 + \varepsilon\sigma, \quad \Omega_2 = \Omega_1 + \varepsilon\Delta. \tag{5}
$$

where σ, Δ are the two independent detuning parameters. Following the multiple scales method [32], equation (4) solutions are presented as

$$
\xi = \xi_0(T_0, T_1, \ldots) + \varepsilon\xi_1(T_0, T_1, \cdots) + \ldots, \tag{6}
$$

where $T_0 = t$, $T_1 = \varepsilon t$. Then two equations are derived:

$$
\frac{\partial^2\xi_0}{\partial T_0^2} + \xi_0 = 0, \tag{7}
$$

$$\frac{\partial^2\xi_1}{\partial T_0^2}+\xi_1=-2\frac{\partial^2\xi_0}{\partial T_0\partial T_1}-\lambda\xi_0^3+\gamma_1\cos\Omega_1T_0+\mu\left[\gamma_2\cos\Omega_2T_0-\tilde{\theta}\ \text{sign}\left(\frac{\partial\xi_0}{\partial T_0}-v_B\right)\right.$$
$$\left.+\tilde{\theta}\alpha\left(\frac{\partial\xi_0}{\partial T_0}-v_B\right)-\tilde{\theta}\beta\left(\frac{\partial\xi_0}{\partial T_0}-v_B\right)^3\right]. \tag{8}$$

The solution of equation (4) is

$$\xi_0=\sqrt{2\rho}\cos(\Omega_1T_0-\theta). \tag{9}$$

The following Fourier series is used:

$$sign\left[\sqrt{2\rho}\sin(\Omega_1t-\theta)+v_B\right]=-\sum_{-\infty}^{\infty}c_n\exp[in(\Omega_1t-\theta)], \tag{10}$$

where

$$c_1=i\alpha_1,\quad \alpha_1=\begin{cases}0, v_B>\sqrt{2\rho},\\ \frac{2}{\pi}\sqrt{1-\frac{v_B^2}{2\rho}}, v_B<\sqrt{2\rho}\end{cases}$$

Neglecting the secular terms from (8), the following system of modulation equations is derived:

$$\rho'=\sqrt{\rho}\frac{\gamma_1}{\sqrt{2}}\sin\theta+\mu\left\{-\tilde{\theta}\alpha_1\sqrt{2\rho}+\rho\tilde{\theta}(\alpha-3\beta v_B^2)-\frac{3}{2}\tilde{\theta}\beta\rho^2+\sqrt{\rho}\frac{\gamma_2}{\sqrt{2}}\sin\theta\cos\Delta T_1\right.$$
$$\left.+\sqrt{\rho}\frac{\gamma_2}{\sqrt{2}}\cos\theta\sin\Delta T_1\right\} \tag{11}$$

$$\theta'=\sigma-\frac{3\lambda}{4}\rho+\frac{\gamma_1}{2\sqrt{2\rho}}\cos\theta+\mu\frac{\gamma_2}{2\sqrt{2\rho}}(\cos\theta\cos\Delta T_1-\sin\theta\sin\Delta T_1). \tag{12}$$

The modulation equations (11 and 12) have both periodic and chaotic motions. As follows from (11) and (12) if $\gamma_2=0$ and the resonance conditions (5) are satisfied, there are not chaotic states in the system (4). If two harmonics of almost periodic excitation are interacted, chaotic motions take place. Note that ε is only a part of modulation equations time scale. Therefore, bifurcations of the system (4) do not depend on ε.

4. Unperturbed Modulation System Analysis

In this section it is considered the unperturbed system (11) and (12) with Hamiltonian:

$$H=-\sqrt{2\rho}\frac{\gamma_1}{2}\cos\theta+\frac{3\lambda}{8}\rho^2-\sigma\rho. \tag{13}$$

The Hamiltonian has two groups of fixed points (θ_1,ρ_1) and (θ_2,ρ_2). which satisfy the equations:

$$\sigma-\frac{3\lambda}{4}\rho_{1,2}\pm\frac{\gamma_1}{2\sqrt{2\rho_{1,2}}}=0,\quad \theta_1=0,\quad \theta_2=\pm\pi. \tag{14}$$

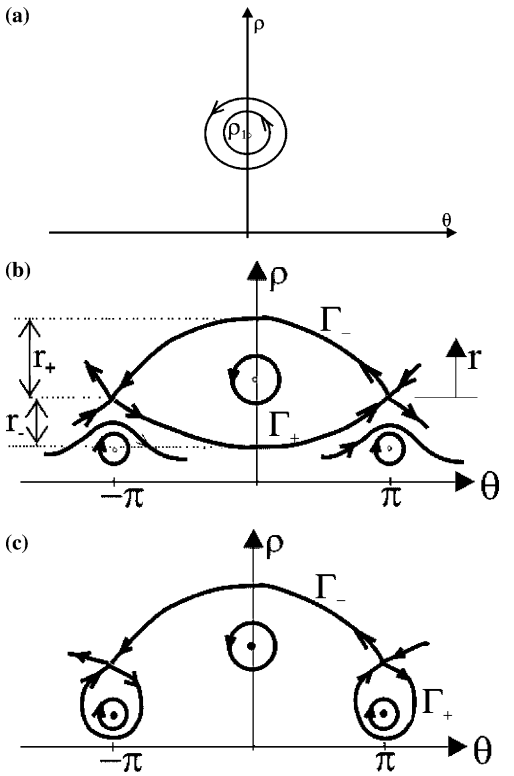

Figure 2. The phase planes of the unperturbed modulation equations. These figures correspond to the following parameters: (a) $-\gamma_1 \succ \frac{8\sqrt{2\sigma^3}}{9\sqrt{\lambda}}$, (b) $-0 \prec \gamma_1 \prec \frac{8}{9}\sqrt{\frac{\sigma^3}{\lambda}}$, (c) $-\frac{8}{9}\sqrt{\frac{\sigma^3}{\lambda}} \prec \gamma_1 \prec \frac{8}{9}\sqrt{\frac{\sigma^3 2}{\lambda}}$.

Note that the values ρ_1 (ρ_2) correspond to plus (minus) sign of equation (14). If the system parameters satisfy the inequality:

$$\gamma_1 > \frac{8\sqrt{2\sigma^3}}{9\sqrt{\lambda}}, \tag{15}$$

then the following fixed point appears:

$$\sqrt{\rho_1} = \sqrt[3]{\frac{\gamma_1}{3\sqrt{2}\lambda}}\left(\sqrt[3]{1-\sqrt{1-\frac{128\sigma^3}{81\lambda\gamma_1^2}}}+\sqrt[3]{1+\sqrt{1-\frac{128\sigma^3}{81\lambda\gamma_1^2}}}\right). \tag{16}$$

The eigenvalues of the linearized flow close to this fixed point are

$$\tilde{\lambda} = \pm \mathrm{i}\sqrt{\frac{\gamma_1}{4\sqrt{2}}\left(3\lambda\sqrt{\rho}+\frac{\gamma_1}{\sqrt{2}\rho}\right)}. \tag{17}$$

Therefore, the fixed point ρ_1 is orbitally stable. The phase trajectories of this case are shown in Figure 2a.

Now the behavior of the unperturbated system (11) and (12) is considered, when the system parameters satisfy the inequality:

$$\gamma_1 < \frac{8\sqrt{2\sigma^3}}{9\sqrt{\lambda}}. \tag{18}$$

Then three fixed points $\rho_1, \rho_2^{(1)}$ and $\rho_2^{(2)}$ in the unperturbated system (11) and (12) exist:

$$\sqrt{\rho_1} = \tilde{c}\cos\left[\frac{1}{3}\arccos\tilde{b}\right]; \sqrt{\rho_2^{(1)}} = \tilde{c}\cos\left[\frac{\pi}{3} - \frac{1}{3}\arccos\tilde{b}\right];$$
$$\sqrt{\rho_2^{(2)}} = \tilde{c}\cos\left[\frac{\pi}{3} + \frac{1}{3}\arccos\tilde{b}\right], \tag{19}$$

where $\tilde{c} = \frac{4}{3}\sqrt{\frac{\sigma}{\lambda}}$, $\tilde{b} = \frac{9\sqrt{\lambda}\gamma_1}{8\sqrt{2}\sigma^{3/2}}$. Now equation (17) is used to study stability of the fixed point ρ_1. The eigenvalues $\tilde{\lambda}$ of the linearized flow are determined to study stability of fixed points $\rho_2^{(1,2)}$:

$$\tilde{\lambda}^2 = \frac{\gamma_1\sqrt{\rho}}{\sqrt{2}}\left(\frac{3\lambda}{4} - \frac{\gamma_1}{4\sqrt{2}\rho^{3/2}}\right). \tag{20}$$

If it is assumed, that the fixed points $\rho_2^{(1)}$ and $\rho_2^{(2)}$ just appear due to the saddle-node bifurcation, then the following inequality is true $\rho_2^{(1)} > \rho_2^{(2)}$. In this case the following relations are met:

$$\frac{8\sqrt{2}\sigma^{3/2}}{9\sqrt{\lambda}} - \tilde{\varepsilon} = \gamma_1, \quad 0 < \tilde{\varepsilon} \ll 1. \tag{21}$$

Then the fixed points are determined as

$$\sqrt{\rho_2^{(1,2)}} = \frac{2}{3}\sqrt{\frac{\sigma}{\lambda}}\left(1 \pm \sqrt{\tilde{\varepsilon}\frac{3\sqrt{\lambda}}{4\sqrt{2\sigma^3}}}\right) + O(\tilde{\varepsilon}), \tag{22}$$

The eigenvalues of the linearized flow close to $\rho_2^{(1)}$ and $\rho_2^{(2)}$ have the following form:

$$\tilde{\lambda}^{(1,2)2} = \pm\frac{\sqrt{3}\gamma_1^2}{4\sqrt{2}\rho}\sqrt{\tilde{\varepsilon}\frac{9\sqrt{\lambda}}{8\sqrt{2\sigma^3}}}, \tag{23}$$

where $\tilde{\lambda}^{(1)}$ corresponds to $\rho_2^{(1)}$. The fixed points $\rho_2^{(2)}$ and $\rho_2^{(1)}$ are orbitally stable (unstable), respectively.

Now the behavior of the unperturbated system (11) and (12) is considered, when the system parameters satisfy the equations:

$$\gamma_1 = \frac{8\sqrt{2\sigma^3}}{9\sqrt{\lambda}}. \tag{24}$$

In this case, the saddle-node bifurcation takes place and two fixed points $\rho_2^{(1)}$ and $\rho_2^{(2)}$ are jointed. The fixed points have the form:

$$\sqrt{\rho_1} = 2\sqrt[3]{\frac{\gamma_1}{3\sqrt{2}\lambda}}, \quad \sqrt{\rho_2^{(1)}} = \sqrt{\rho_2^{(2)}} = \frac{\sqrt{\rho_1}}{2}. \tag{25}$$

Hamiltonian (13) of the orbitally stable fixed point $(\theta_1 = 0, \rho_1)$ has the value:

$$H_C^{(1)} = -\frac{2\sqrt{\rho_1 \sigma^3}}{3\sqrt{\lambda}} \left[2\cos^2\left(\frac{1}{6}\arccos\tilde{b}\right) - \delta \right], \tag{26}$$

where $\tilde{b} = 1 - \delta$. The parameter δ defines the distance of the unperturbated system from the saddle-node bifurcation. The value of the Hamiltonian in the saddle-point ($\theta_2 = \pi, \rho_2^{(1)}$) is

$$H_S = \frac{2\sqrt{\rho_2^{(1)} \sigma^3}}{3\sqrt{\lambda}} \left[2\sin^2\left(\frac{\pi}{6} - \frac{1}{6}\arccos\tilde{b}\right) - \delta \right] \tag{27}$$

and the value of the Hamiltonian in the orbitally stable fixed point $(\theta_2 = \pi, \rho_2^{(2)})$ is

$$H_c^{(2)} = \frac{2\sqrt{\rho_2^{(2)} \sigma^3}}{3\sqrt{\lambda}} \left[2\sin^2\left(\frac{\pi}{6} + \frac{1}{6}\arccos\tilde{b}\right) - \delta \right]. \tag{28}$$

Fixed points and separatrixes are a skeleton of phase portraits of the unperturbated system. To obtain qualitatively the behavior of the separatrixes at different values of the system parameters the intersections of the separatrixes with the line $\theta = \pi$ (see Figure 2) is found. These intersections are described by the equation, which follows from (13). The condition of the existence of the second positive root of this equation is: $\gamma_1 < \frac{8}{9}\sqrt{\frac{\sigma^3}{\lambda}}$. Thus, the phase portraits of the unperturbated system at $0 < \gamma_1 < \frac{8}{9}\sqrt{\frac{\sigma^3}{\lambda}}$ and $\frac{8}{9}\sqrt{\frac{\sigma^3}{\lambda}} < \gamma_1 < \frac{8}{9}\sqrt{\frac{\sigma^3 2}{\lambda}}$ differ qualitatively and they are shown in Figure 2b and c, respectively. Note that the separatrixes are denoted by $\Gamma_-(\rho_-(t); \theta_-(t))$ and $\Gamma_+(\rho_+(t); \theta_+(t))$ (see Figure 2).

Let us determine these separatrixes for the case (Figure 2b). The following formula is derived from equation (12): $\theta_\pm(t) = \arcsin\left(\frac{\sqrt{2}\rho'_\pm}{\gamma_1\sqrt{\rho_\pm}}\right)$. which is substituted into (13). After some algebra the following result is derived:

$$\rho'^2 = \left(\frac{\gamma_1\sqrt{\rho}}{\sqrt{2}} + \sigma\rho - \frac{3\lambda}{8}\rho^2 + H_s\right)\left(\frac{\gamma_1\sqrt{\rho}}{\sqrt{2}} - \sigma\rho + \frac{3\lambda}{8}\rho^2 - H_s\right). \tag{29}$$

The change of the variables: $\rho(t) = \rho_2^{(1)} + r(t)$ and the initial conditions:

$$\theta_\pm(0) = 0, \quad \rho_\pm(0) = \rho_2^{(1)} + \tilde{r}_\pm. \quad \tilde{r}_\pm = 2(k \pm \sqrt{2k\rho_2^{(1)}}), \quad k = \frac{4\sigma}{3\lambda} - \rho_2^{(1)}$$

are used to integrate the equation (11). As a result, the function $\rho_\pm(t)$ is derived as

$$\rho_\pm(t) = \rho_2^{(1)} \pm \frac{2\tilde{r}_-\tilde{r}_+}{(\tilde{r}_+ - \tilde{r}_-)\cosh(\tilde{a}T_1) \pm (\tilde{r}_+ + \tilde{r}_-)}, \quad \tilde{a} = \frac{3\lambda}{8}\sqrt{-\tilde{r}_-\tilde{r}_+}. \tag{30}$$

5. Almost Periodic Motions

Almost periodic motions of the system (4) correspond to the periodic solutions of the system (11) and (12). These motions close to the fixed points of the unperturbated system (11) and (12) are investigated in this section.

The change of the variables is introduced:

$$\rho(t)=\rho_2^{(2)}+\mu\eta(t),\quad \theta(t)=\pi+\mu\varphi(t). \tag{31}$$

As $\mu\ll 0$. the periodic motions close to the saddle fixed point $(\rho_2^{(1)},\pi)$ are unstable. In this section stability and bifurcations of the motions close to the stable fixed point $(\rho_2^{(2)},\pi)$ are studied by the approach suggested by Holmes, and Holmes [42]. The functions $\eta(t)$ and $\varphi(t)$ (31) satisfy the following differential equations:

$$\begin{aligned}\eta' &= -\frac{\gamma_1}{\sqrt{2}}\sqrt{\rho_2^{(2)}}\varphi + A^{(1)} - \sqrt{\frac{\rho_2^{(2)}}{2}}\gamma_2\sin(\Delta T_1),\\ \varphi' &= \left(\frac{\gamma_1}{4\rho_2^{(2)}\sqrt{2\rho_2^{(2)}}} - \frac{3\lambda}{4}\right)\eta - \frac{\gamma_2}{2\sqrt{2\rho_2^{(2)}}}\cos(\Delta T_1).\end{aligned} \tag{32}$$

The solution of this system is

$$\eta=\frac{h}{\lambda_2^2-\Delta^2}\cos(\Delta T_1),\quad \varphi=\frac{\sqrt{2}}{\gamma_1\sqrt{\rho_2^{(2)}}}\left(\frac{h\Delta}{\lambda_2^2-\Delta^2}-\sqrt{\frac{\rho_2^{(2)}}{2}}\gamma_2\right)\sin(\Delta T_1)+\tilde{A}^{(1)}, \tag{33}$$

where the parameters $\lambda_2, w, \tilde{A}^{(1)}$ are presented in Appendix A. The following change of the variables is used:

$$\rho=\rho_2^{(2)}+\sqrt{\mu}h(T_1)+\mu\eta(T_1),\quad \theta=\pi+\sqrt{\mu}\psi+\mu\varphi. \tag{34}$$

Then the non-linear differential equations are derived:

$$\begin{aligned}\dot{h} = &-\frac{\gamma_1}{\sqrt{2}}\sqrt{\rho_2^{(2)}}\psi - \sqrt{\mu}\gamma_1\frac{h\psi}{2\sqrt{2\rho_2^{(2)}}} + \mu\left\{h\left[A^{(2)}-\frac{\gamma_1\varphi}{2\sqrt{2\rho_2^{(2)}}}-\frac{\gamma_2}{2\sqrt{2\rho_2^{(2-)}}}\sin(\Delta T_1)\right]\right.\\ &\left.-\psi\left[\sqrt{\rho_2^{(2)}}\frac{\gamma_2}{\sqrt{2}}\cos(\Delta T_1)+\frac{\gamma_1\eta}{2\sqrt{2\rho_2^{(2)}}}\right]+\frac{\gamma_1\sqrt{\rho_2^{(2)}}}{6\sqrt{2}}\psi^3+\frac{\gamma_1 h^2\psi}{8\sqrt{2}\rho_2^{(2)3/2}}\right\},\end{aligned} \tag{35}$$

$$\begin{aligned}\dot{\psi} = &\left(\frac{\gamma_1}{4\rho_2^{(2)}\sqrt{2\rho_2^{(2)}}}-\frac{3\lambda}{4}\right)h+\sqrt{\mu}\frac{\gamma_1}{2\sqrt{2\rho_2^{(2)}}}\left(\frac{\psi^2}{2}-\frac{3h^2}{8\rho_2^{(2)2}}\right)+\mu\left\{\frac{\gamma_1}{2\sqrt{2\rho_2^{(2)}}}\right.\\ &\left.\left(\psi\varphi-\frac{h\psi^2}{4\rho_2^{(2)}}-\frac{3h\eta}{4\rho_2^{(2)}}\right)+\frac{\gamma_2}{2\sqrt{2\rho_2^{(2)}}}\left(\psi\sin(\Delta T_1)+\frac{h}{2\rho_2^{(2)}}\cos(\Delta T_1)\right)\right\},\end{aligned} \tag{36}$$

where the parameter $A^{(2)}$ and the function $\beta_1(\rho_2^{(2)})$ are presented in Appendix A. The main parametric resonance in the system (35) and (36) is considered:

$$\mu\sigma_2=\frac{\Delta^2}{4}-\lambda_2^2. \tag{37}$$

where σ_2 is a detuning parameter. Then the frequencies Ω_1 and Ω_2 satisfy the following equation:

$$\Omega_2 = \Omega_1 + \varepsilon 2\lambda_2 + \varepsilon\mu\frac{\sigma_2}{\lambda_2} + O(\varepsilon\mu^2).$$

The change of the variables

$$\begin{aligned} h &= u\cos\left(\frac{\Delta}{2}T_1\right) - v\sin\left(\frac{\Delta}{2}T_1\right), \\ \frac{\gamma_1}{\Delta}\sqrt{2\rho_2^{(2)}}\psi &= u\sin\left(\frac{\Delta}{2}T_1\right) + v\cos\left(\frac{\Delta}{2}T_1\right) \end{aligned} \tag{38}$$

is used to study the system (35) and (36). Then the system (35) and (36) is rewritten with respect to u, v and the average procedure is carried out. As a result the following equations are derived:

$$\begin{aligned} \dot{u} = \mu\Bigg\{&\left[f_1\cos\frac{\Delta}{2}T_1\right]_0 + \frac{\gamma_1}{\Delta}\sqrt{2\rho_2^{(2)}}\left[f_2\sin\frac{\Delta}{2}T_1\right]_0 + \frac{\sigma_2}{\Delta}v + \frac{u^2 v}{256\Delta\rho_2^{(2)2}} \\ &\times\left(6\Delta^2 - \frac{6\gamma_1^2}{\rho_2^{(2)}} + \frac{15\gamma_1^4}{2\Delta^2\rho_2^{(2)2}}\right) + \frac{3v^3}{256\Delta\rho_2^{(2)2}}\left(2\Delta^2 + \frac{5\gamma_1^4}{2\Delta^2\rho_2^{(2)2}} - \frac{2\gamma_1^2}{\rho_2^{(2)}}\right)\Bigg\}, \end{aligned} \tag{39}$$

$$\begin{aligned} \dot{v} = \mu\Bigg\{&\frac{\gamma_1}{\Delta}\sqrt{2\rho_2^{(2)}}\left[f_2\cos\frac{\Delta}{2}T_1\right]_0 - \left[f_1\sin\frac{\Delta}{2}T_1\right] - \sigma_2\frac{u}{\Delta} - \frac{uv^2}{256\rho_2^{(2)2}\Delta} \\ &\times\left(6\Delta^2 + \frac{15\gamma_1^4}{2\Delta^2\rho_2^{(2)2}} - \frac{6\gamma_1^2}{\rho_2^{(2)}}\right) - \frac{3u^3}{256\rho_2^{(2)2}\Delta}\left(2\Delta^2 + \frac{5\gamma_1^4}{2\Delta^2\rho_2^{(2)2}} - \frac{2\gamma_1^2}{\rho_2^{(2)}}\right)\Bigg\}, \end{aligned} \tag{40}$$

where $[\ ]_0$ is the average operator. The system (39) and (40) has the following form:

$$\begin{aligned} \dot{u} &= \mu\left\{D_1 u + \left(D_2 + \frac{\sigma_2}{\Delta}\right)v + D(u^2 v + v^3)\right\}, \\ \dot{v} &= \mu\left\{u\left(-\frac{\sigma_2}{\Delta} + D_2\right) + D_1 v - D(u^3 + v^2 u)\right\}, \end{aligned} \tag{41}$$

where the parameters $D_1, D_2, \chi.D$ are presented in Appendix A. The system (41) is rewritten with respect to the variables $(R^2.\gamma) = \left(u^2 + v^2, \operatorname{arctg}\left(\frac{v}{u}\right)\right)$:

$$\dot{R} = \mu(D_1 R + D_2 R\sin 2\gamma), \quad \dot{\gamma} = \mu\left(D_2\cos 2\gamma - DR^2 - \frac{\sigma_2}{\Delta}\right). \tag{42}$$

This dynamical system has three groups of the fixed points R_1, R_2, R_3:

$$R_{1,2'}^2 = -\frac{\sigma_2}{D\Delta} \pm \frac{1}{D}\sqrt{\gamma_2^2\chi^2 - D_1^2}, \quad R_3 = 0. \tag{43}$$

Note, that the following inequalities are true:

$$D\Delta < 0, \quad D_1 < 0. \tag{44}$$

These fixed points are presented qualitatively on the bifurcation diagram (Figure 3), where R versus σ_2 are shown. The eigenvalues $(\pi_1.\pi_2)$ of the linearized flow are

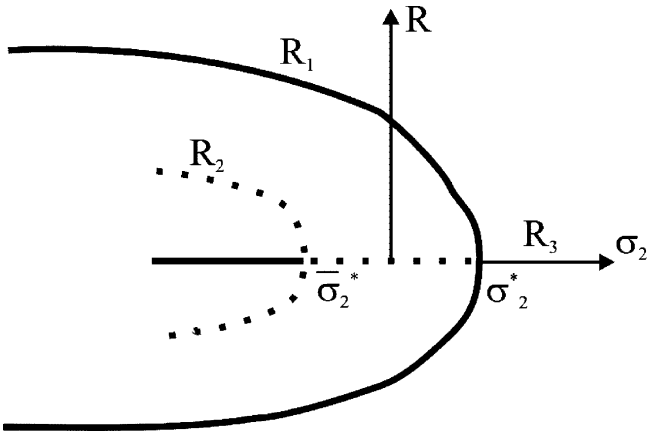

Figure 3. Qualitatively bifurcation diagram of the fixed points, where R versus σ_2 are shown.

derived to study stability of these points. The eigenvalues $(\pi_1^{(3)}, \pi_2^{(3)})$ of the vector field close to the fixed point R_3 are

$$\pi_1^{(3)} = D_1 + \sqrt{D_2^2 - \frac{\sigma_2^2}{\Delta^2}}, \quad \pi_2^{(3)} = -2\sqrt{D_2^2 - \frac{\sigma_2^2}{\Delta^2}}. \tag{45}$$

As follows from (45), the boundary of stability/ instability is

$$\sigma_2^{\bullet} = 2\lambda_2\sqrt{\gamma_2^2\chi^2 - D_1^2}, \quad \tilde{\sigma}_2^{\bullet} = -\sigma_2^{\bullet}. \tag{46}$$

These values are shown in Figure 3, where the stable (unstable) motions are presented by solid (dotted) line, respectively. The stability of the fixed points R_1 is described by the eigenvalues:

$$\pi_{1,2}^{(1)} = D_1 \pm \sqrt{D_1^2 - 4DR_1^2\sqrt{\gamma_2^2\chi^2 - D_1^2}} < 0. \tag{47}$$

Thus, the fixed points R_1 are stable. The eigenvalues $(\pi_1^{(2)}.\pi_2^{(2)})$ of the fixed points R_2 are

$$\pi_{1,2}^{(2)} = D_1 \pm \sqrt{D_1^2 + 4DR_2^2\sqrt{\gamma_2^2\chi^2 - D_1^2}}. \tag{48}$$

The values $\pi_{1,2}^{(2)}$ meet the inequalities: $\pi_1^{(2)} > 0, \quad \pi_2^{(2)} < 0$ and the fixed points R_2 are unstable.

Now the bifurcation behavior of the fixed points is considered. The pitchfork bifurcations (Figure 3) occur at $\sigma_2 = \sigma_2^{\bullet}$ and $\sigma_2 = \tilde{\sigma}_2^{\bullet}$. The location of these bifurcations satisfies the equation:

$$\gamma_2^2\chi^2 - \frac{\sigma_2^2}{4\lambda_2^2} = D_1^2. \tag{49}$$

Equation (49) describes a hyperbola, which is denoted by (AC_1B) (see Figure 4). The codimension two bifurcation point C_1 joints two pitchfork bifurcations and has

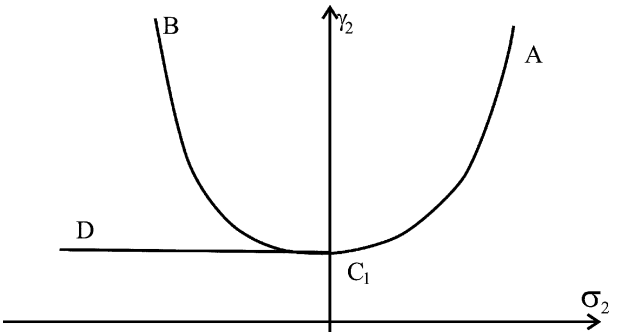

Figure 4. The bifurcation curves on the plane (σ_2, γ_2). The pitchfork bifurcation curve and saddle-node bifurcation curve are denoted by (AC_1B) and (C_1D). respectively.

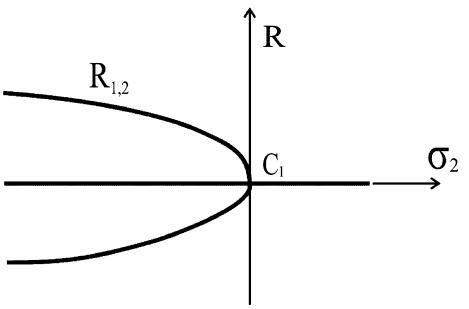

Figure 5. The bifurcation diagram $R-\sigma_2$ containing the point C_1.

the following coordinates on plane (σ_2, γ_2) : $C_1(0; \bar{\gamma}_2)$, $\bar{\gamma}_2 = D_1/\chi$. At $\bar{\gamma} = \bar{\gamma}_2$ two branches of bifurcation diagram $R_1 - \sigma_2$ and $R_2 - \sigma_2$ merge and the saddle-node bifurcation line is formed. The saddle-node bifurcation curve meets the equation:

$$R_{1,2}^2 = -\frac{\sigma_2}{D\Delta}. \tag{50}$$

The bifurcation diagram $R-\sigma_2$ with the point C_1 is shown in Figure 5. The saddle-node bifurcation set is a straight line on the plane (σ_2, γ_2) (see Figure 4).

The variables $(R,\ \gamma)$ and the variables of the system (4) are connected as:

$$\xi = -\sqrt{2\rho_2^{(2)}}\cos\Omega_1 t - \sqrt{\mu}R\left[\frac{\Delta}{\gamma_1}\sin\Omega_1 t \sin\left(\frac{\Delta}{2}\varepsilon t + \gamma\right)\right.$$
$$\left. + \frac{1}{\sqrt{2\rho_2^{(2)}}}\cos\Omega_1 t \cos\left(\frac{\Delta}{2}\varepsilon t + \gamma\right)\right] + O(\mu) + O(\varepsilon). \tag{51}$$

Now the system (4) oscillations are considered. The fixed points $R_3 = 0$ correspond to the stable oscillations of the system (4) with period $T_1 = 2\pi/\Omega_1$. The fixed points R_1 and R_2 correspond to the almost periodic oscillations (51).

6. Chaotic Solutions of the Modulation Equations

An appearance of the heteroclinic tangency is chosen as the criterion of chaotic oscillations. The Melnikov function $\tilde{M}$ is calculated to analyze a heteroclinic tangency

[41] and the applications of this functions to discontinuous systems are considered in the papers [43, 44]. Taking into account the equations (11) and (12), the Melnikov heteroclinic function is derived as

$$\tilde{M}=\int_{-\infty}^{\infty}\left\{-\frac{\gamma_1\gamma_2}{4}\sin\theta\cos(\Delta t-\Delta t_0+\theta)+\frac{\gamma_2}{\sqrt{2}}\sqrt{\rho}\sin(\Delta t-\Delta t_0+\theta)\right.$$
$$\left.\times\left(\sigma-\frac{3}{4}\lambda\rho+\frac{\gamma_1}{2\sqrt{2\rho}}\cos\theta\right)\right\}\mathrm{d}t+\int_{-\infty}^{\infty}\mathrm{P}(\rho)\left(\sigma-\frac{3}{4}\lambda\rho+\frac{\gamma_1}{2\sqrt{2\rho}}\cos\theta\right)\mathrm{d}t, \quad (52)$$

where $\mathrm{P}(\rho)=-\tilde{\theta}\alpha_1\sqrt{2\rho}+\rho\tilde{\theta}(\alpha-3\beta v_B^2)-\frac{3}{2}\tilde{\theta}\beta\rho^2$. The integration (52) is carried out along the trajectories of the unperturbed system taking into account the relations: $\rho(t)=\rho(-t), \quad \theta(t)=-\theta(-t)$. After some algebra the heteroclinic Melnikov function is obtained as

$$\tilde{M}=\frac{\gamma_2}{2}\sin(\Delta t_0)\left\{\int_{-\infty}^{\infty}\left(-\sigma\sqrt{2\rho}\cos\theta+\frac{3\lambda}{4}\rho\sqrt{2\rho}\cos\theta-\frac{\gamma_1}{2}\right)\cos(\Delta t)\mathrm{d}t\right.$$
$$+\sigma\int_{-\infty}^{\infty}\sqrt{2\rho}\sin\theta\sin(\Delta t)\mathrm{d}t-\frac{3\lambda}{4}\int_{-\infty}^{\infty}\rho\sqrt{2\rho}\sin\theta\sin(\Delta t)\mathrm{d}t\Big\}$$
$$+\int_{-\infty}^{\infty}\mathrm{P}(\rho)\left(\sigma-\frac{3}{4}\lambda\rho+\frac{\gamma_1}{2\sqrt{2\rho}}\cos\theta\right)\mathrm{d}t. \quad (53)$$

The equation: $\cos\theta=\sqrt{\frac{2}{\rho\gamma_1^2}}\left(\frac{3\lambda}{8}\rho^2-\sigma\rho-H_S\right)$ is used to calculate the Melnikov function. As a result it is derived

$$\tilde{M}_{\pm}(t_0)=\frac{\gamma_2}{2}A_{\pm}\sin(\Delta t_0)+D_{\pm}. \quad (54)$$

The derivation of $D_{\pm}$ and the value $A_{\pm}$ are given in Appendix B. The parameter $A_{\pm}$ contains the following integrals:

$$K_n^{\pm}=\int_{-\infty}^{\infty}r_{\pm}^n(t)\cos(\Delta t)\mathrm{d}t, \quad L_n^{\pm}=\int_{-\infty}^{\infty}r_{\pm}^n(t)\dot{r}_{\pm}(t)\sin(\Delta t)\mathrm{d}t, \quad n=1,2,3. \quad (55)$$

The integrals (55) satisfy the following equations:

$$L_0=-\Delta K_1, \quad K_2=-\frac{2}{\Delta}L_1. \quad (56)$$

The following values of the integrals (55) are derived by the residues method:

$$K_1^{\pm}=\mp\frac{16\pi\sinh(\tilde{\Delta}\theta_0^{\pm})}{3\lambda\sinh(\tilde{\Delta}\pi)}, K_2^{\pm}=\frac{16\pi\tilde{\rho}}{3\lambda}\left[\tilde{\Delta}\frac{\cosh(\tilde{\Delta}\theta_0^{\pm})}{\sinh(\tilde{\Delta}\pi)}\mp\mathrm{ctg}\theta_0\frac{\sinh(\tilde{\Delta}\theta_0^{\pm})}{\sinh(\tilde{\Delta}\pi)}\right],$$

$$K_3^{\pm}=\mp\frac{8\pi\tilde{\rho}^2}{3\lambda\sinh(\tilde{\Delta}\pi)}\left\{\sinh(\tilde{\Delta}\theta_0^{\pm})(1+3\mathrm{ctg}^2\theta_0+\tilde{\Delta}^2)\mp3\tilde{\Delta}ctg\theta_0\cosh(\tilde{\Delta}\theta_0^{\pm})\right\},$$

$$L_0^{\pm}=\pm\frac{16\Delta\pi\sinh(\tilde{\Delta}\theta_0^{\pm})}{3\lambda\sinh(\tilde{\Delta}\pi)}, L_1^{\pm}=-\frac{8\Delta\pi\tilde{\rho}}{3\lambda}\left[\Delta'\frac{\cosh(\tilde{\Delta}\theta_0^{\pm})}{\sinh(\tilde{\Delta}\pi)}\mp\mathrm{ctg}\theta_0\frac{\sinh(\tilde{\Delta}\theta_0^{\pm})}{\sinh(\tilde{\Delta}\pi)}\right],$$

where $\tilde{\Delta} = 8\Delta/3\tilde{\rho}\lambda$. The formulae for $\theta_0^{\pm}, \tilde{\rho}$ and $A_{\pm}(\Delta, \lambda, \gamma_1, \sigma)$ are presented in Appendix B.

If the equation $\tilde{M}_{\pm} = 0$ has the simple roots, the upper and lower invariant manifolds Γ_+ and Γ_- (Figure 2b) are intersected transversally and the Smale horseshoes take place [41]. If the inequality

$$\left|\frac{D_{\pm}}{A_{\pm}}\right| < \frac{\gamma_2^{(\pm)}}{2} \tag{57}$$

satisfies, the transversal intersections of the invariant manifolds occur in the system (4). The boundary of the region (57) satisfies the equation:

$$\gamma_2^{(\pm)} = 2\left|\frac{D_{\pm}(\beta, v_B, \alpha, \tilde{\theta}, \lambda, \sigma, \gamma_1)}{A_{\pm}(\Delta, \lambda, \gamma_1, \sigma)}\right|. \tag{58}$$

The boundary (58) is considered on the parameter plane (Δ, γ_2). The right part of equation (58) does not depend on γ_2. Moreover, the numerator of the right part does not depend on Δ. For future analysis the value $A_{\pm}$ is rewritten in the form, which contains explicit dependence on Δ (see Appendix B). Using these relations, the following limits are derived:

$$\lim_{\Delta\to\infty}\gamma_2^{(\pm)} = \infty, \quad \lim_{\Delta\to-\infty}\gamma_2^{(\pm)} = \infty, \lim_{\Delta\to 0}\gamma_2^{(\pm)} = \left|\frac{16\pi D_{\pm}}{9\tilde{\rho}\lambda\ \mathrm{const}_1 \mp 8\theta_0^{\pm}\ \mathrm{const}_2}\right|, \tag{59}$$

where const_1 and const_2 are presented in Appendix 2. The numerical calculations are performed to analyze the boundary (58). The numerical values of the system (1) parameters are taken from the book [5]:

$$m = 0.981\mathrm{kg}, \quad c = 9.81\times 10^3 \tfrac{\mathrm{N}}{\mathrm{m}}, \quad c_3 = 1.67\times 10^3 \tfrac{\mathrm{N}}{\mathrm{m}^3}, \quad \Gamma_1 = 100\,\mathrm{N}, \quad \theta_0 = 4.9\mathrm{N},$$
$$A = 0.2\tfrac{\mathrm{kg}}{\mathrm{sec}}, \quad B = 3\times 10^{-6}\tfrac{\mathrm{kg}\times\mathrm{sec}}{\mathrm{m}^2}.$$

Then the dimensionless parameters of the system (4) are the following:

$$\varepsilon = 0.01, \quad \mu = 0.1, \quad \lambda = 17, \quad \tilde{\theta} = 0.5, \quad \gamma_1 = 1.02, \quad \alpha = 4.08, \quad \beta = 0.61,$$
$$\sigma = 10, \quad v_B = 4.$$

The boundaries of the heteroclinic orbits intersections $\gamma_2^{(+)}(\Delta)$ and $\gamma_2^{(-)}(\Delta)$ are shown in Figure 6a and b, respectively.

7. Numerical Analysis of Modulation Equations

In this section it is reported the numerical results of the steady states bifurcations in the modulation equations (11) and (12), when γ_2 is changed and $\Delta = 1.944$. The values of γ_2 are taken with some steps and the system (11) and (12) is solved by the Runge–Kutta method. The numerical integration is carried out with different initial values to determine the main steady states of the system. The integration is performed until the dynamical system reaches a steady state. Afterwards, the initial conditions are changed and the integration is repeated.

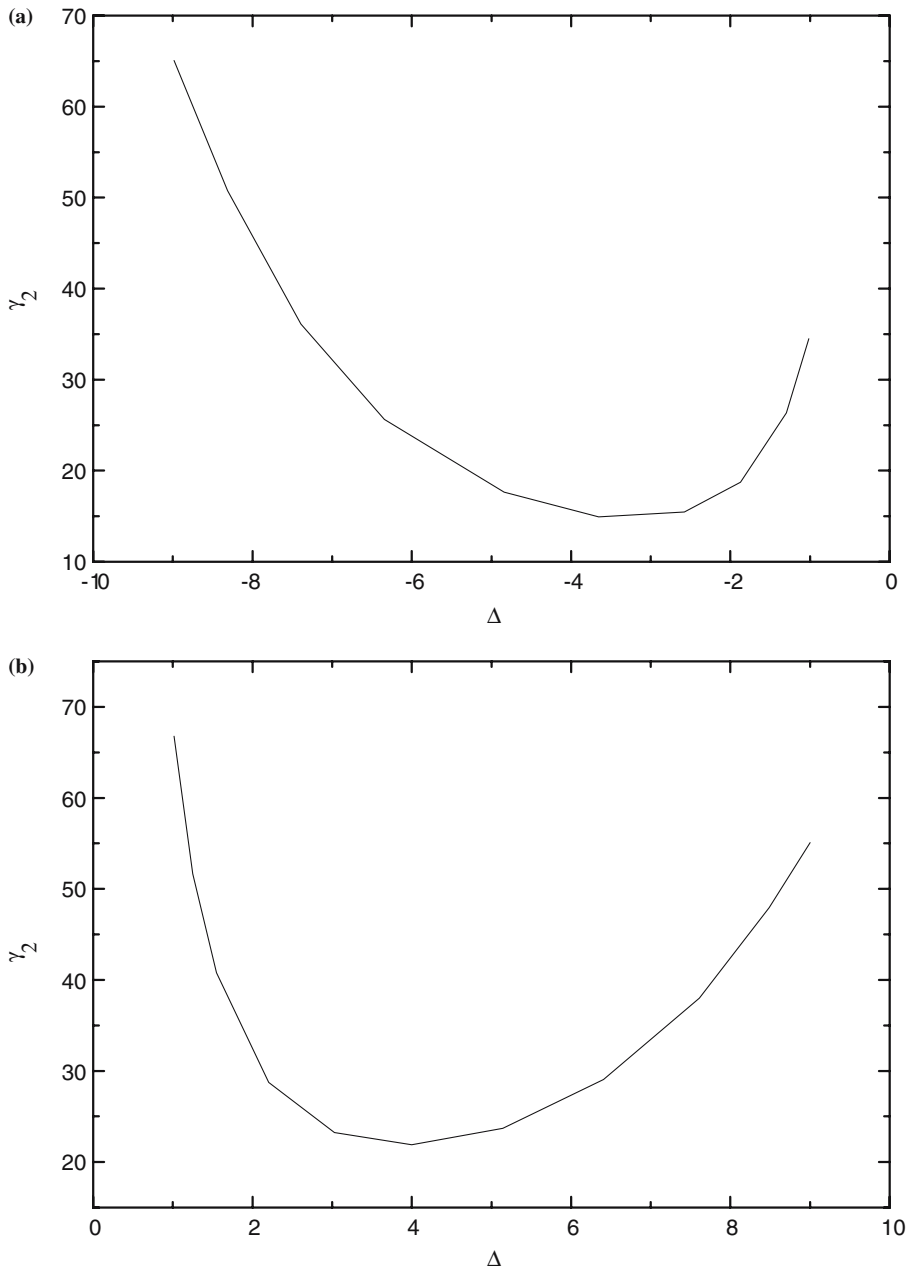

Figure 6. The boundaries of the heteroclinic orbits intersections. (a) $\gamma_2^{(+)}(\Delta)$. (b) $\gamma_2^{(-)}(\Delta)$.

The following dynamical behavior of the system (11) and (12) is discovered. The limit cycles of the period $T_1 = 2\pi\ \Delta^{-1}$ are observed in $\gamma_2 \in [10; 43]$. These limit cycles take place close to the fixed point ρ_1 of the unperturbated system (11) and (12). For example, the limit cycle at $\gamma_2 = 43$ is shown in Figure 7a. The period-doubling bifurcation occurs at the interval $\gamma_2 \in [43; 44]$ and the limit cycle period is doubled. Such limit cycle at $\gamma_2 = 46$ is shown in Figure 7b. These motions exist in the wide range $\gamma_2 \in [46; 74]$. In this interval the additional limit cycles exist at some parameters. The

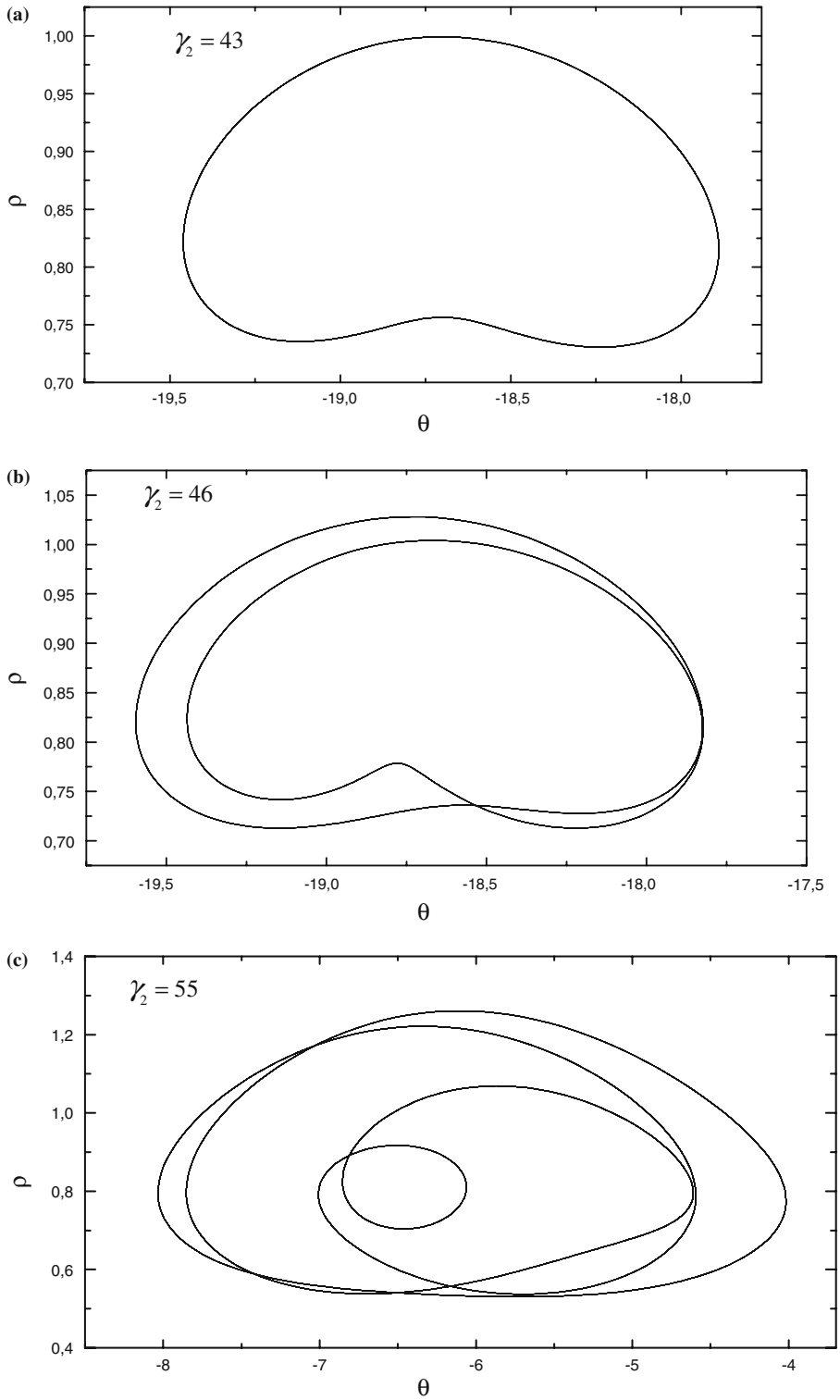

Figure 7. The limit cycles obtained by the numerical calculations.

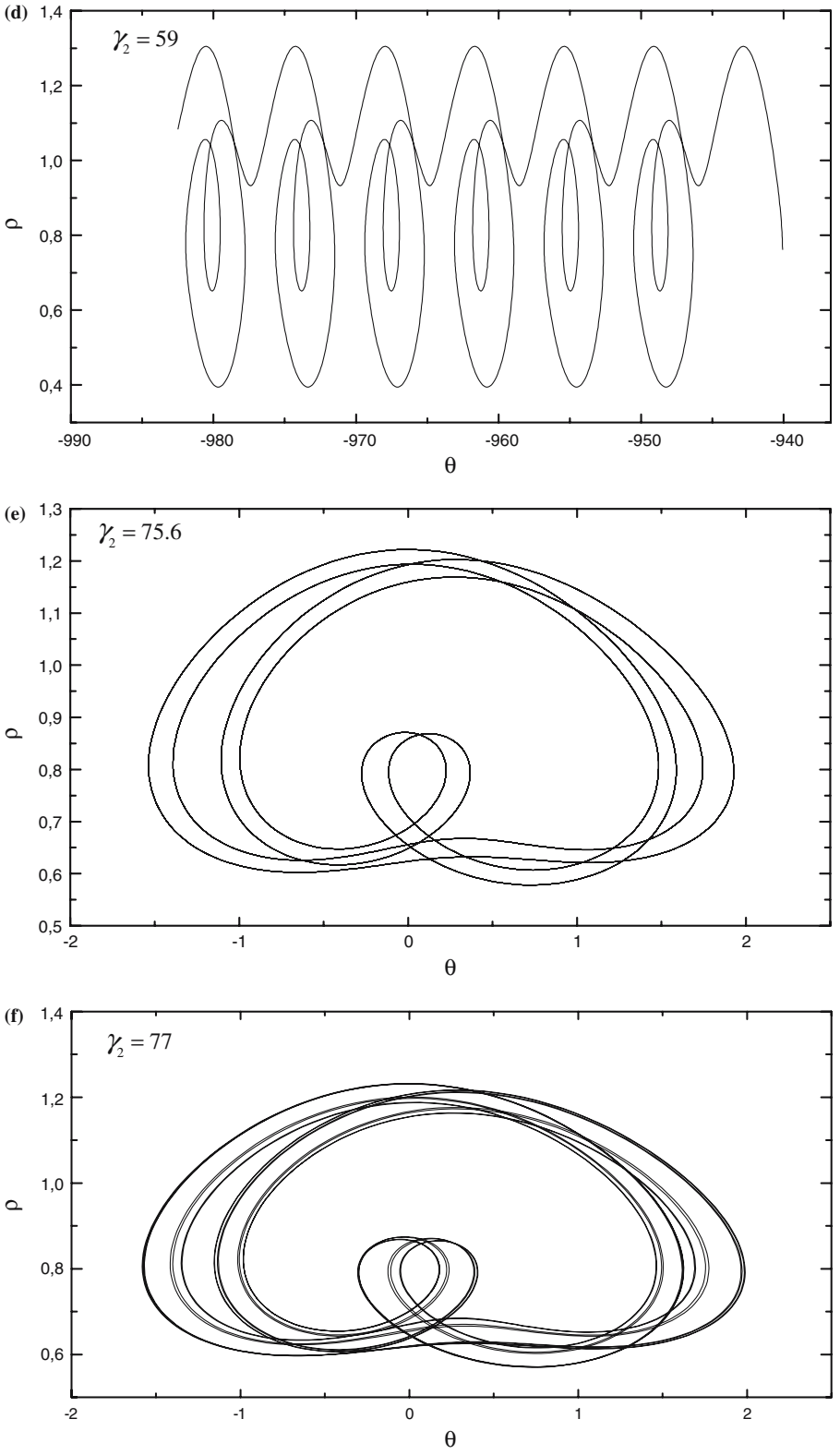

Figure 7. continued

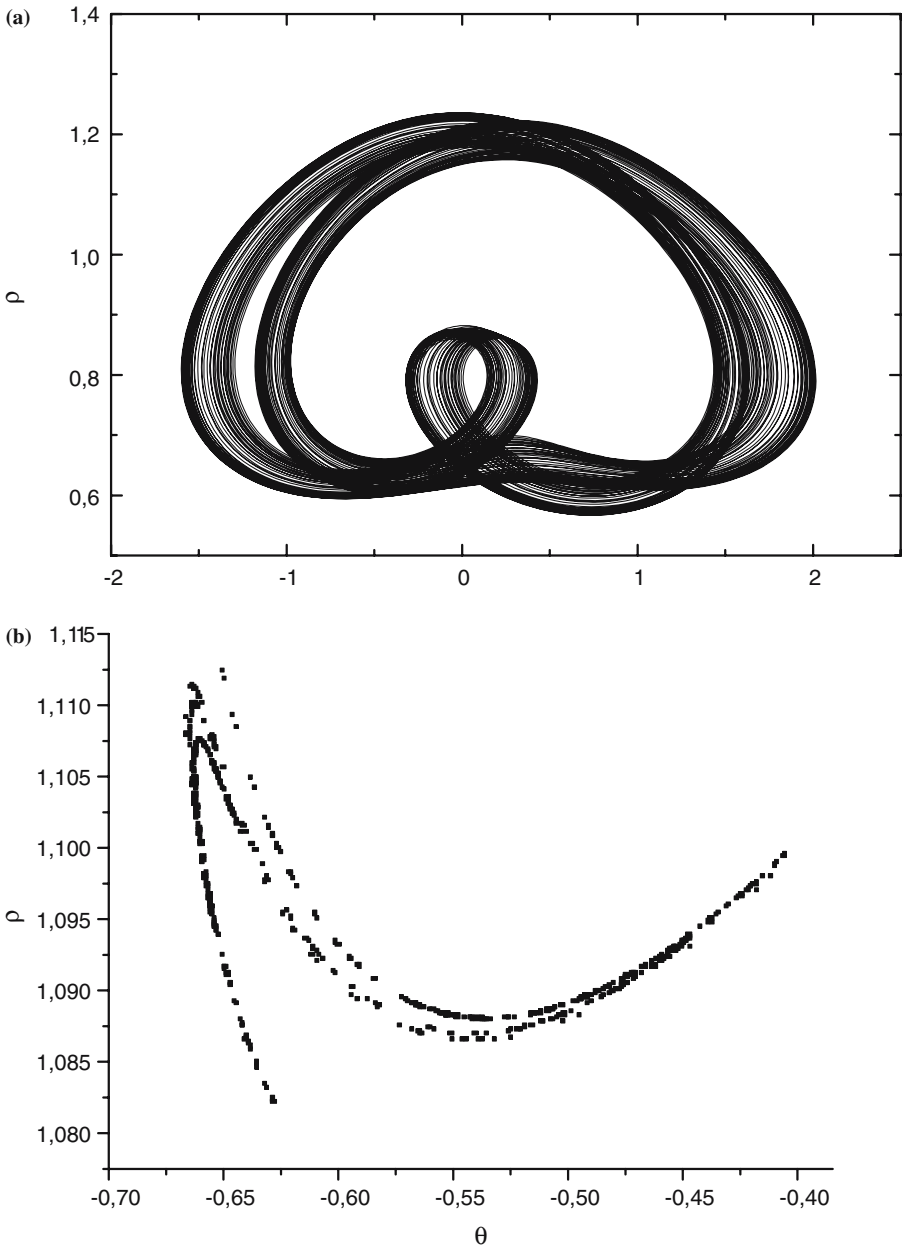

Figure 8. Chaotic attractor and its Poincare map at $\gamma_2 = 77.3$.

third order limit cycle is observed at $\gamma_2 = 55$ (Figure 7c). This motion is discovered close to the heteroclinic trajectories of the unperturbated modulation equations. The theory of these motions is based on the subharmonic Melnikov functions [41, 45]. According to this theory the limit cycle is arisen due to the saddle-node bifurcation. The complex periodic motion (Figure 7d) was observed besides the second order limit cycle at $\gamma_2 = 59$.

The period- doubling bifurcation takes place in the interval $\gamma_2 \in [74; 75.5]$ and the fourth order limit cycle is arisen (Figure 7e). This motion undergoes the period- doubling bifurcation and the 8^{th} order limit cycle appear. This cycle is shown in Figure 8f at $\gamma_2 = 77$. The chaotic attractors take place if γ_2 is increased slightly. For example, such attractor is shown in Figure 8a at $\gamma_2 = 77.3$. The Poincare sections of this attractor are shown in Figure 8b.

Thus, the system behavior predicted by means of the heteroclinic Melnikov function is verified by the numerical integration. All limit cycles considered here correspond to the almost periodic oscillations of the system (4).

8. Conclusions

The frictional oscillations have been considered in this paper. As the oscillator is disposed on the moving belt, the energy of this belt is pumped over to the oscillator. The actions of almost periodic excitations on the system have been considered. The heteroclinic Melnikov function has been obtained to study the region of the chaotic oscillations in the periodically excited system. The system of the modulation equations has been derived by the multiple scales method for the almost periodically excited system. The bifurcations behavior is studied analytically in the system of the modulation equations. The heteroclinic Melnikov function has been used to analyze the region of the chaotic solutions existence of the modulation equations. The numerical analysis of the modulation equations, which confirms the chaotic dynamics, has been presented. It has been shown, that the chaotic motions are arisen due to the sequence of the periodic-doubling bifurcations.

Acknowledgement

The first author express thanks to Professors Yu. V. Mikhlin, F. Pellicano, O. Morachkovski for many useful conversations on the topics presented in this article. A financial support of a visit to the Department of Automatics and Biomechanics (Technical University of Lodz, Poland) within this research subject is also acknowledged by the first author of this paper.

Appendix A

$$\lambda_2^2 = \frac{\gamma_1^2}{8\rho_2^{(2)}} - \frac{3\lambda\gamma_1}{4\sqrt{2}}\sqrt{\rho_2^{(2)}}, \quad w = \frac{\gamma_1\gamma_2}{4} - \sqrt{\frac{\rho_2^{(2)}}{2}}\gamma_2\Delta, \quad \tilde{A}^{(1)} = A^{(1)}\frac{\sqrt{2}}{\gamma_1\sqrt{\rho_2^{(2)}}},$$

$$A^{(2)} = \tilde{\theta}\left[-\frac{\alpha_1(\rho_2^{(2)})}{\sqrt{2\rho_2^{(2)}}} - \sqrt{2\rho_2^{(2)}}\beta_1(\rho_2^{(2)}) + \alpha - 3\beta\nu_B^2 - 3\beta\rho_2^{(2)}\right],$$

$$\beta_1(\rho_2^{(2)}) = \begin{cases} 0, & v_B > \sqrt{2\rho_2^{(2)}}, \\ \dfrac{2v_B^2}{\left(2\rho_2^{(2)}\right)^{3/2}\pi\sqrt{2\rho_2^{(2)} - v_B^2}}, & v_B < \sqrt{2\rho_2^{(2)}}. \end{cases}$$

$$D_1 = \frac{B_1}{2} + \frac{\gamma_1\tilde{A}^{(1)}}{4\sqrt{2\rho_2^{(2)}}} = \frac{A^{(2)}}{2}, \quad D_2 = \frac{B_2}{2} - \frac{B_3\Delta}{4\gamma_1\sqrt{2\rho_2^{(2)}}} + \frac{\gamma_1\sqrt{2\rho_2^{(2)}}B_4}{4\Delta} = \gamma_2\chi,$$

$$\chi = \frac{1}{4\sqrt{2\rho_2^{(2)}}} - \frac{\lambda_2}{4\gamma_1} + \frac{\gamma_1^3}{256\rho_2^{(2)}\lambda_2^3} - \frac{\sqrt{2}\gamma_1^2}{64\sqrt{\rho_2^{(2)}}\lambda_2^2},$$

$$D = \frac{1}{16^2\rho_2^{(2)2}\Delta}\left[\Delta^2 + \frac{13\gamma_1^4}{2\Delta^2\rho_2^{(2)2}} + \left(3\Delta - \frac{\gamma_1^2}{\Delta\rho_2^{(2)}}\right)^2 + \frac{4\Delta^4\rho_2^{(2)}}{\gamma_1^2}\right],$$

$$f_1 = h\left[B_1 - B_2\sin\Delta T_1\right] - \psi B_3\cos\Delta T_1 + \frac{\gamma_1\sqrt{\rho_2^{(2)}}}{6\sqrt{2}}\psi^3 + \frac{\gamma_1 h^2\psi}{8\sqrt{2}\rho_2^{(2)3/2}},$$

$$f_2 = B_2\psi\sin\Delta T_1 + B_4 h\cos\Delta T_1 + \frac{\gamma_1\tilde{A}^{(1)}}{2\sqrt{2\rho_2^{(2)}}}\psi - \frac{\gamma_1 h\psi^2}{8\rho_2^{(2)}\sqrt{2\rho_2^{(2)}}},$$

$$\Lambda_1 = \frac{W}{\lambda_2^2 - \Delta^2} = -\frac{\gamma_2}{3\lambda_2^2}\left(\frac{\gamma_1}{4} - \lambda_2\sqrt{2\rho_2^{(2)}}\right), \quad B_1 = A^{(2)} - \frac{\gamma_1\tilde{A}^{(1)}}{2\sqrt{2\rho_2^{(2)}}},$$

$$B_2 = \frac{\gamma_1\Lambda_2 + \gamma_2}{2\sqrt{2\rho_2^{(2)}}} = \frac{\gamma_2}{6\sqrt{2\rho_2^{(2)}}}\left(4 - \frac{\gamma_1}{\lambda_2\sqrt{2\rho_2^{(2)}}}\right),$$

$$B_3 = \sqrt{\rho_2^{(2)}}\frac{\gamma_2}{\sqrt{2}} + \frac{\gamma_1}{2\sqrt{2\rho_2^{(2)}}}\Lambda_1 = \gamma_2\left[\sqrt{\frac{\rho_2^{(2)}}{2}} + \frac{\gamma_1}{6\sqrt{2\rho_2^{(2)}}\lambda_2^2}\left(\lambda_2\sqrt{2\rho_2^{(2)}} - \frac{\gamma_1}{4}\right)\right],$$

$$B_4 = \frac{2\gamma_2 - 3\Lambda_1\gamma_1}{8\rho_2^{(2)}\sqrt{2\rho_2^{(2)}}} = \frac{\gamma_2}{8\rho_2^{(2)}\sqrt{2\rho_2^{(2)}}}\left(2 + \frac{\gamma_1^2}{4\lambda_2^2} - \frac{\gamma_1}{\lambda_2}\sqrt{2\rho_2^{(2)}}\right).$$

Appendix B

$$D_{\pm}=\frac{1}{2}\left(3\beta v_B^2-\alpha\right)\tilde{\theta}\int_{-\infty}^{\infty}2\rho_{\pm}\left(-\sigma+\frac{3\lambda}{4}\rho_{\pm}-\frac{\gamma_1\cos\theta_{\pm}}{2\sqrt{2\rho_{\pm}}}\right)\mathrm{d}t$$
$$+\int_{-\infty}^{\infty}\left(-\tilde{\theta}\alpha_1\sqrt{2\rho_{\pm}}-\frac{3}{2}\tilde{\theta}\beta\rho_{\pm}^2\right)\left(\sigma-\frac{3}{4}\lambda\rho_{\pm}+\frac{\gamma_1}{2\sqrt{2\rho_{\pm}}}\cos\theta_{\pm}\right)\mathrm{d}t$$

$$=\pm6\int_{\tilde{r}_{\mp}}^{0}\frac{r\mathrm{d}r}{\sqrt{(r-\tilde{r}_-)(\tilde{r}_+-r)}}\pm\frac{16}{3\lambda}\left(\frac{9\lambda}{4}\rho_2^{(1)}-\sigma\right)\int_{\tilde{r}_{\mp}}^{0}\frac{\mathrm{d}r}{\sqrt{(r-\tilde{r}_-)(\tilde{r}_+-r)}}$$
$$+\frac{3}{2}\tilde{\theta}\beta\left\{\frac{9}{16}\lambda\int_{-\infty}^{\infty}r_{\pm}^3\mathrm{d}t+\left(\frac{27}{16}\lambda\rho_2^{(1)}-\frac{\sigma}{2}\right)\int_{-\infty}^{\infty}r_{\pm}^2\mathrm{d}t+\rho_2^{(1)}\left(\frac{9}{8}\lambda\rho_2^{(1)}-\frac{\sigma}{2}\right)\int_{-\infty}^{\infty}r_{\pm}\mathrm{d}t\right\}$$
$$+\int_{-\infty}^{\infty}\tilde{\theta}\alpha_1\sqrt{2\rho_{\pm}}\left(-\sigma+\frac{3}{4}\lambda\rho_{\pm}-\frac{\gamma_1}{2\sqrt{2\rho_{\pm}}}\cos\theta_{\pm}\right)$$
$$\mathrm{d}t=\mp\left(3\beta v_B^2-\alpha\right)\tilde{\theta}\frac{16}{3\lambda}\left(\sigma\theta_0^{\pm}\mp\frac{9\lambda}{16}\tilde{\rho}\right)$$

$$+\tilde{\theta}\beta\left\{\frac{14\tilde{\rho}\sigma}{\lambda}\mp\theta_0^{\pm}\left[\left(9\rho_2^{(1)}-\frac{4\sigma}{\lambda}\right)\left(\frac{4\sigma}{\lambda}-2\rho_2^{(1)}\right)+\frac{7\sigma(\tilde{r}_++\tilde{r}_-)}{\lambda}\right]\right\}+\tilde{\theta}\frac{9\lambda}{16}J_2^{(\pm)}$$
$$+\tilde{\theta}\left(\frac{9}{8}\lambda\rho_2^{(1)}-\frac{\sigma}{2}\right)J_1^{(\pm)},$$

where $\theta_0^+=\theta_0$, $\quad\theta_0^-=\pi-\theta_0$, $\quad\theta_0=\arccos\left(\frac{\tilde{r}_++\tilde{r}_-}{\tilde{r}_+-\tilde{r}_-}\right)$, $\quad\tilde{\rho}=\sqrt{-\tilde{r}_+\tilde{r}_-}$,

$$J_j^{(-)}=\begin{cases}\dfrac{32\sqrt{2}}{3\lambda\pi}\displaystyle\int_0^{\tilde{r}_+}\frac{r^{j-1}\sqrt{\rho_2^{(1)}-\frac{v_B^2}{2}+r}\mathrm{d}r}{(\rho_2^{(1)}+r)\sqrt{(r-\tilde{r}_-)(\tilde{r}_+-r)}}, & \dfrac{v_B^2}{2}-\rho_2^{(1)}<0,\\ \dfrac{32\sqrt{2}}{3\lambda\pi}\displaystyle\int_{\frac{v_B^2}{2}-\rho_2^{(1)}}^{\tilde{r}_+}\frac{r^{j-1}\sqrt{\rho_2^{(1)}-\frac{v_B^2}{2}+r}\mathrm{d}r}{(\rho_2^{(1)}+r)\sqrt{(r-\tilde{r}_-)(\tilde{r}_+-r)}}, & 0<\dfrac{v_B^2}{2}-\rho_2^{(1)}<\tilde{r}_+,\\ 0, & \dfrac{v_B^2}{2}-\rho_2^{(1)}<\tilde{r}_+,\end{cases}$$

$$J_j^{(+)}=\begin{cases}\dfrac{32\sqrt{2}}{3\lambda\pi}\displaystyle\int_0^{\tilde{r}_-}\frac{r^{j-1}\sqrt{\rho_2^{(1)}-\frac{v_B^2}{2}+r}\mathrm{d}r}{(\rho_2^{(1)}+r)\sqrt{(r-\tilde{r}_-)(\tilde{r}_+-r)}}, & \tilde{r}_-<\dfrac{v_B^2}{2}-\rho_2^{(1)},\\ \dfrac{32\sqrt{2}}{3\lambda\pi}\displaystyle\int_{\frac{v_B^2}{2}-\rho_2^{(1)}}^{\tilde{r}_-}\frac{r^{j-1}\sqrt{\rho_2^{(1)}-\frac{v_B^2}{2}+r}\mathrm{d}r}{(\rho_2^{(1)}+r)\sqrt{(r-\tilde{r}_-)(\tilde{r}_+-r)}}, & \tilde{r}_-<\dfrac{v_B^2}{2}-\rho_2^{(1)}<0,\\ 0, & \dfrac{v_B^2}{2}-\rho_2^{(1)}<0,\end{cases}$$

$j = 1, 2.$

$$A_{\pm}(\Delta, \lambda, \gamma_1, \sigma) = \frac{9\lambda^2}{16\gamma_1} K_3^{\pm} - \frac{9\lambda}{8\gamma_1}(2\sigma - \frac{3}{2}\rho_2^{(1)}\lambda) K_2^{\pm} - \frac{1}{2\gamma_1}$$
$$\left[\frac{9}{4}\gamma_1\lambda\sqrt{2\rho_2^{(1)}} - \sigma(4\sigma - 3\lambda\rho_2^{(1)})\right] K_1^{\pm} - \frac{3\lambda}{2\gamma_1} L_1^{\pm} + \left(\frac{2\sigma}{\gamma_1} - \frac{3\lambda}{2\gamma_1}\rho_2^{(1)}\right) L_0^{\pm},$$

$$A_{\pm}(\Delta, \lambda, \gamma_1, \sigma) = \cos\text{ech}\left(\frac{8\Delta\pi}{3\tilde{\rho}\lambda}\right)\left\{\mp\frac{8\pi\Delta}{3\lambda\gamma_1}\left(\frac{3}{2}\lambda\tilde{\rho}\,\text{ctg}\theta_0 - 2\left[2\sigma - \frac{3}{2}\lambda\rho_2^{(1)}\right]\right)\right.$$
$$+\frac{2\pi}{3\lambda\gamma_1}\left\{\frac{27}{4}\lambda^2\tilde{\rho}^2\text{ctg}^2\theta_0 - 9\lambda\tilde{\rho}(2\sigma - \frac{3}{2}\rho_2^{(1)}\lambda)\text{ctg}\ \theta_0 - 9\gamma_1\lambda\sqrt{2\rho_2^{(1)}}\right.$$
$$\left.+8\sigma(2\sigma - \frac{3}{2}\rho_2^{(1)}\lambda) + \frac{9}{4}\lambda^2\tilde{\rho}^2\right\} + \frac{\pi\Delta^2 32}{3\gamma_1\lambda}\Big]\sinh(\Delta'\theta_0^{\pm})$$
$$\left.+\left[\frac{\Delta^2\pi 32}{3\gamma_1\lambda} + \frac{8\pi\Delta}{\lambda\gamma_1}\left\{\frac{3}{2}\tilde{\rho}\lambda\text{ctg}\theta_0 - 2(2\sigma - \frac{3}{2}\rho_2^{(1)}\lambda)\right\}\right]\cosh(\Delta'\theta_0^{\pm})\right\}.$$

$$A_{\pm} = \cos\text{ech}\left(\frac{8\Delta\pi}{3\tilde{\rho}\lambda}\right)\left\{\mp\left[\Delta\text{const}_1 + \text{const}_2 + \frac{\pi\Delta^2 32}{3\gamma_1\lambda}\right]\sinh\left(\tilde{\Delta}\theta_0^{\pm}\right) + \left[\frac{\Delta^2\pi 32}{3\gamma_1\lambda}\right.\right.$$
$$\left.\left.+3\Delta\ \text{const}_1\right]\cosh\left(\tilde{\Delta}\theta_0^{\pm}\right)\right\},$$

where

$$\text{const}_1(\lambda, \gamma_1, \sigma) = \frac{8\pi}{3\lambda\gamma_1}\left(\frac{3}{2}\lambda\tilde{\rho}\,\text{ctg}\theta_0 - 2\left[2\sigma - \frac{3}{2}\lambda\rho_2^{(1)}\right]\right),$$

$$\text{const}_2(\lambda, \gamma_1, \sigma) = \frac{2\pi}{3\lambda\gamma_1}\left\{\frac{27}{4}\lambda^2\tilde{\rho}^2\text{ctg}^2\theta_0 - 9\lambda\tilde{\rho}\left(2\sigma - \frac{3}{2}\rho_2^{(1)}\lambda\right)\text{ctg}\theta_0 - 9\gamma_1\lambda\sqrt{2\rho_2^{(1)}}\right.$$
$$\left.+8\sigma\left(2\sigma - \frac{3}{2}\lambda\rho_2^{(1)}\right) + \frac{9}{4}\lambda^2\tilde{\rho}^2\right\}.$$

References

1. Den Hartog J.P., *Mechanical Vibrations*, Mc Graw Hill, New on Dover, 1985.
2. Andronov, A.A., Vitt, A.A. and Khaikin, S.E., *Theory of Oscillations*, Pergamon Press, 1966.
3. Kauderer, H., *Nonlinear Mechanics*, Springer- Verlag, Berlin, 1958 (in German).
4. Kononenko, V.O., Frictional auto-oscillations close to harmonic. Transactions of civil engineering institute of USSR Academy of Science 1954, N9 (in Russian).
5. Kononenko, V.O., *Vibrating Systems with a Limiting Power Supply*, Iliffe, London, 1956.
6. Alifov, A.A. and Frolov, K.V., *Interactions of the Nonlinear Systems with Energy Sources*, Moscow, Nauka, 1964 (in Russian).
7. Popp, K. and Stelter, P., 'Stick-slip vibrations and chaos', *Phil. Trans. R. Soc. Lond. A* **332** (1990) 89–105.
8. Oestreich, M., Hinrichs, N. and Popp, K., 'Bifurcation and stability analysis for a non-smooth friction oscillator', *Arch. Appl. Mech.* **66** (1996) 301–304.
9. Feeny, B. and Moon, F.C., 'Chaos in a forced dry-friction oscillator: experiment and numerical modeling', *J. Sound Vib.* **170**(3) (1994) 303–323.

10. Feeny, B.F. and Moon, F.C., Bifurcation Sequences of a Columb friction oscillator. *Nonlinear Dynam* **4** (1993) 25–37.
11. Wojewoda, J. and Kapitaniak, T. 'Oscillations of a quasi-periodically forced system with dry friction', *J. Sound Vib.* **163**(2) (1993) 379–384.
12. Wojewoda, J., Barron, R. and Kapitaniak, T., 'Chaotic behavior of friction force', *Int J. Bifurcation Chaos* **2**(1) (1992) 205–209.
13. Popp, K. and Stelter, P., 'Nonlinear Oscillations of Structures Induced by Dry Friction', in: Schiehlen, W. (ed.), *Nonlinear Dynamics in Engineering, IUTAM Symposium*, Stuttgart, 1989, pp. 233–240.
14. Awrejcewicz, J. and Delfs, J., 'Dynamics of a self-exicted stick-slip oscillator with two degrees of freedom. Part 1: Investigation of equilibria', *Euro. J. Mech. A/Solids* **9**(4) (1990) 269–282.
15. Awrejcewicz, J. and Delfs, J. 'Dynamics of a self-exicted stick-slip oscillator with two degrees of freedom. Part 2: Slip-stick, slip-slip, stick-slip transitions, periodic and chaotic orbits', *Eur. J. Mech. A/Solids* **9**(5) (1990) 397–418.
16. Awrejcewicz, J. and Holicke, M.M., 'Melnikov's method and stick-slip chaotic oscillations in very weakly forced mechanical systems', *Int. J. Bifurcation Chaos* **9**(3) (1999) 505–518.
17. Awrejcewicz, J. and Olejnik, P., 'Stick-slip dynamics of a two-degree-of-freedom system', *Int. J. Bifurcation Chaos* **13**(4) (2003) 397–418.
18. Awrejcewicz, J., Dzyubak, L. and Grebogi, C., 'A direct numerical method for quantifying regular and chaotic orbits', *Chaos, Solitons and Fractals* **19**(3) (2004) 503–507.
19. Awrejcewicz, J. and Dzyubak, L., 'Stick-slip chaotic oscillations in a quasi-autonomous mechanical system', *Int. J. Nonlinear Sci. Numer. Simul.* **4**(2) (2003) 155–160.
20. Awrejcewicz, J. and Pyryev, Yu., 'Thermo elastic contact of a rotating shaft with a rigid bush in conditions of bush wear and stick-slip movements', *Int. J. Eng. Sci.* **40** (2002) 1113–1130.
21. Awrejcewicz, J. and Pyryev, Yu., Tribological periodic processes exhibited by acceleration or braking of a shaft-pad system', *Commun. Nonlinear Sci. Numer. Simul.* (to appear).
22. Awrejcewicz, J. and Lamarque, C.-H., *Bifurcation and Chaos in Nonsmooth Mechanical Systems*, World Scientific, Singapore, 2003.
23. Bogacz, R., and Ryczek B. 'Friction phenomena in a system with external excitation', in 6th *Conference on Dynamical Systems Theory and Applications* 2001, Lodz, December.
24. Balandin, D.B., 'Frictional Auto-oscillations in clearance', *Mech. Solids* (*Proc. Russian Acad. Sci.*) (1) (1993) 54–60 (in Russian).
25. Marjuta, A.N., 'Analysis of motions of mechanical systems with frictional interaction', *Int. Appl. Mech.* **25**(10) (1989) 84–95.
26. Landa, P.S., *Auto-oscillations of the Systems with Finite Degree of Freedom*, Nauka, Moscow 1980 (in Russian).
27. Pfeiffer, F., 'Complementary problems of stick-slip vibrations', *J. Vib. Acoustic.* **118** (1996) 423–434.
28. Sinou, J., Thouverez, F., Jezequel, L., *Stability Analysis and Application of the Center Manifold Theory for a Nonlinear Sprag-slip Model*. IMAC-XX, Los Angeles, California, 2002.
29. Sinou, J., Thouverez, F., Jezequel, L. and Mazet, G.-B., 'Friction, instability and parametric studies of a nonlinear model for a aircraft brake whirl analysis. *ASME Design Engineering, Technical Conference and Computers and Information* Pittsburg, 2001.
30. Kragelskii, I.V., *Friction and Wear*, Butterworths, Washington 1965.
31. Feeny, B., Guran, A., Hinrichs, N. and Popp, K., 'An historica review on friction in nonlinear dynamics', *App. Mech. Rev.* **51**(5) (1998) 321–341.
32. Malkin, I.G., *Some Problems in the Theory of Nonlinear Oscillations*, GITTL, Moscow, 1956 (in Russian).
33. Nayfeh, A.H. and Mook, D.T., *Nonlinear Oscillations*, Wiley, New York, 1979, p. 704.
34. Vavriv, D.M., Ryabov, V.B., Sharapov, S.A. and Ito H.M. 'Chaotic states of weakly and strongly nonlinear oscillators with quasiperiodic excitation', *Phys. Rev. E* **53**(1) 103–113.
35. Wiggins, S. 'Chaos in quasiperiodically forced Duffing oscillator', *Phys. Lett. A.* **124**(3) (1987).
36. Ide, K., Wiggins, S., 'The bifurcation to harmonic tori in the quasiperiodically forced Duffing oscillator', *Phys. D* **34** (1989) 169–182.
37. Yagasaki, K., 'Chaotic dynamics of a quasi-periodically forced beam', *ASME J. Appl. Mech.* **59** (1992) 123–130.

38. Yagasaki, K., 'Bifurcations and chaos in a quasi-periodically forced beam: theory, simulation and experiment', *J. Sound Vib*. **183**(1) (1995) 1–31.
39. Yagasaki, K., 'Chaotic motions near homoclinic manifolds and resonant tori in quasiperiodic perturbations of planar Hamiltonian systems', *Phys. D.* 69 (1993) 232–269.
40. Wiggins, S, *Global Bifurcations and Chaos-Analytical Methods*, Springer-Verlag, New York, 1988.
41. Guckenheimer J. and Holmes, P., *Nonlinear Oscillations, Dynamical Systems and Bifurcations of Vector Fields*, Springer-Verlag, New York, 1983.
42. Holmes, C. and Holmes, P.J. 'Second order averaging and bifurcations to subharmonic in Duffing's equation', *J. Sound Vib.* **78** (1981) 161–174.
43. Chow, S.N. and Shaw S.W., *Bifurcations of subharmonics*', *J. Differ. Eq.* **65**(3) (1986) 304–320.
44. Shaw, S.W. and Rand R.H., 'The transition to Chaos in a simple mechanical system. I', *J. Non- Linear Mech.* **24**(1) 41–56.
45. Avramov, K.V., 'Bifurcations of parametric oscillations of beams with three equilibria', *Acta Mechanica* (2003).